A composite biochemical system for bacterial nitrate and nitrite assimilation as exemplified by Paracoccus denitrificans

Andrew J Gates, Victor Luque-Almagro, Alan Goddard, Stuart John Ferguson, María Dolores Roldán, David J Richardson

Biochemical Journal Immediate Publication. Published on 24 Feb 2011 as manuscript BJ20101920

A composite biochemical system for bacterial nitrate and nitrite assimilation as exemplified by *Paracoccus denitrificans*

Andrew J. Gates*†[1], Victor M. Luque-Almagro‡[1], Alan D. Goddard§, Stuart J. Ferguson§, M. Dolores Roldán‡, David J. Richardson*†[2]

*Centre for Molecular and Structural Biochemistry, University of East Anglia, Norwich Research Park, Norwich, NR4 7TJ, UK., †School of Biological Sciences, University of East Anglia, Norwich Research Park, Norwich, NR4 7TJ, UK., ‡Departamento de Bioquímica y Biología Molecular, Universidad de Córdoba, Edificio Severo Ochoa, 1ª planta, Campus de Rabanales, Córdoba, 14071, Spain., §Department of Biochemistry, University of Oxford, South Parks Road, Oxford, OX1 3QU, UK.

[1]The authors have contributed equally to this work.

[2]To whom correspondence should be addressed (d.richardson@uea.ac.uk).

Running title: Nitrate and nitrite assimilation in *Paracoccus denitrificans*.

Keywords: nitrate reductase, nitrite reductase, nitrate transport, *Paracoccus denitrificans*.

Abbreviations used: Nas, assimilatory nitrate reductase; Nar, membrane-bound nitrate reductase; Nap, periplasmic nitrate reductase; FAD, flavin-adenine dinucleotide; NAD(P)$^+$ and NAD(P)H, oxidized and reduced nicotinamide-adenine dinucleotide (phosphate); MV, Methyl Viologen; K_M, Michaelis constant; O.D., optical density; $\mu_{max(app)}$, apparent maximum growth rate.

The denitrifying bacterium *Paracoccus denitrificans* can grow aerobically or anaerobically using nitrate or nitrite as the sole N-sources. The biochemical pathway responsible is expressed from a gene cluster comprising a: nitrate/nitrite transporter (NasA), nitrite transporter (NasH), nitrite reductase (NasB), ferredoxin (NasG) and nitrate reductase (NasC). NasB and NasG are essential for growth with nitrate or nitrite as N-source. NADH serves as electron-donor for nitrate and nitrite reduction, but only NasB has a NADH-oxidising domain. Nitrate and nitrite reductase activities show the same K_M for NADH and can be separated by anion-exchange chromatography, but only fractions containing NasB retain the ability to oxidise NADH. This implies that NasG mediates electron-flux from the NADH-oxidising site in NasB to the sites of nitrate and nitrite reduction in NasC and NasB, respectively. Delivery of extracellular nitrate to NasBGC is mediated by NasA, but both NasA and NasH contribute to nitrite uptake. The roles of NasA and NasC can be substituted during anaerobic growth by the biochemically-distinct membrane-bound respiratory nitrate reductase (Nar), demonstrating functional overlap. *nasG* is highly conserved in nitrate/nitrite assimilation gene clusters, consistent with a key role for the NasG ferredoxin, as part of a phylogenetically widespread composite nitrate and nitrite reductase system.

INTRODUCTION

The importance of inorganic nitrate as a key nutritional component of the global nitrogen cycle, particularly for marine and freshwater autotrophic phytoplankton is long recognised. This highly soluble anion can make a significant environmental impact, supporting accelerated biomass formation or 'blooms' in nitrate and phosphate polluted water courses that may have an important role as CO_2 sinks. Accordingly, the biochemistry of nitrate assimilation has been well studied in cyanobacteria where assimilatory nitrate reduction is functionally linked to photosynthetic processes, and both nitrate and nitrite reductases use photosynthetically reduced ferredoxin as

electron donor. By contrast, the utilisation of nitrate by heterotrophic bacteria has received less attention. The ability of heterotrophic bacteria and archaea to metabolise nitrate or nitrite as the sole nitrogen source (N-source) for growth is phylogenetically widespread. However, only a few physiological, genetic and biochemical studies have been performed, most notably early studies on *Enterobacter aerogenes* [1] and more recent studies on the γ-proteobacterium *Klebsiella oxytoca* [2], the photoheterotroph *Rhodobacter capsulatus* [3], the Gram positive bacterium *Bacillus subtilis* [4] and the diazotroph *Azotobacter vinelandii* [5]. In contrast to cyanobacteria the reductases from most heterotrophic bacteria are thought to be dependent on the cytoplasmic reduced pyridine nucleotide pool, which enables them to be coupled to organic carbon catabolism [6]. In fact, recent data suggest heterotrophic bacterial species that can utilise nitrate for the biosynthesis of essential cellular components during growth may also be significant consumers of inorganic nitrogen globally, particularly in environments where there are high concentrations of dissolved organic carbon relative to dissolved organic nitrogen [7-9]. This is due to the high bioenergetic demand for reducing equivalents required for the assimilatory reduction of nitrate to ammonia, which requires eight electrons:

$$NO_3^- + 2H^+ + 2e^- \rightarrow NO_2^- + H_2O \qquad \text{Equation 1}$$

$$NO_2^- + 8H^+ + 6e^- \rightarrow NH_4^+ + 2H_2O \qquad \text{Equation 2}$$

Consequently assimilatory nitrate reduction is a good route for disposal of the excess reductant present in a reduced organic carbon pool [10]. However, the biochemical mechanism by which bacterial assimilatory nitrate reductases access this pool of cellular reductant is not well understood, particularly because analysis of the primary structure of heterotrophic bacterial assimilatory nitrate reductases suggests that they do not have a NAD(P)H binding domain [2, 11].

In addition to being a substrate for nitrogen assimilation in heterotrophs, nitrate can also be a substrate for anaerobic respiration, for example in denitrifying bacteria that can reduce nitrate, via nitrite, nitric oxide and nitrous oxide, to dinitrogen gas and enterobacteria that can reduce nitrate to ammonium [1, 12]. One of the paradigm heterotrophic denitrifiers, *Paracoccus denitrificans* synthesises two heterotrimeric respiratory ubiquinol/nitrate oxidoreductases, Nar and Nap (Fig. 1). The membrane-bound enzyme (NarGHI) reduces nitrate as the first step of growth-linked anaerobic denitrification while the other, a periplasmic system (NapABC), serves to dissipate excess reducing equivalents formed during aerobic growth [12, 13]. These enzymes have been studied at the biochemical level and derive electrons from the membrane-confined ubiquinol pool [14, 15], which can be coupled to NADH generated from oxidative metabolism via the NADH-ubiquinone oxidoreductase. In *P. denitrificans* NarGHI, the active site for nitrate reduction is exposed to the cytoplasm and therefore it is dependent on a nitrate transport protein NarK, a fusion protein of two transmembrane domains NarK1 and NarK2, to deliver nitrate into the cell (Fig. 1). These two functional components have putative roles in nitrogen oxyanion trafficking: NarK1 is a proposed proton-linked nitrate importer, and NarK2 is a putative nitrate/nitrite antiporter [16, 17].

Paracoccus species can also assimilate nitrate via a third cytoplasmic reductase that has not yet been characterised, but is known to be distinct from the two respiratory systems [18]. In general, a bacterial nitrate assimilation system (Nas) involves a cytoplasmic molybdenum-dependent nitrate reductase that reduces nitrate to nitrite (Equation 1), which is further reduced to ammonium by a sirohaem-dependent nitrite reductase (Equation 2) [2]. Like the respiratory Nar system, the cytoplasmic assimilatory system is also dependent on nitrate transport into the cell. However, a major biochemical conundrum is that it is not clear how the assimilatory nitrate reductase is coupled to NADH oxidation. This is because primary sequence analysis of bacterial assimilatory nitrate reductases suggests that, in contrast to the nitrite reductases, they do not possess an NADH binding

domain [2, 11]. The absence of such a site is unimportant for photoautotrophic metabolism in cyanobacteria, where the electron donor is ferredoxin that is photoreduced by photosystem I [19], but it is an important issue in organoheterotrophic metabolism where the nitrate reductase needs to be coupled to NADH released from oxidative metabolism of organic substrates. In this study we identify a key role for a putative Rieske-type [2Fe-2S] ferredoxin in *P. denitrificans* that is widely conserved in other bacterial Nas systems and show that this protein is essential for coupling of NADH oxidation to both nitrate and nitrite reduction. A three-component ferredoxin-nitrate-nitrite reductase system is proposed, where the ferredoxin mediates electron transfer from a single NADH-oxidising site within the nitrite reductase to the sites of nitrate and nitrite reduction present in the nitrite reductase and nitrate reductase components, respectively. Bioinformatic analysis of *nas* gene clusters suggests that this is a widespread mechanism amongst heterotrophic bacterial species and so provides the biochemical link between the nitrate reductase and the cytoplasmic NADH pool. In addition we demonstrate a degree of biochemical overlap between the assimilatory Nas system and the respiratory Nar system at the level of nitrate transport and reduction.

EXPERIMENTAL

Bacterial strains, media and growth conditions

All bacterial strains and plasmids used in this study are listed in Table 1. *P. denitrificans* was routinely cultured under aerobic conditions at 30 ^{o}C in either Luria-Bertani (LB) medium or a defined mineral salts medium with 50 mM succinate as the carbon source [20, 21]. Ammonium chloride (10 mM), potassium nitrate (20 mM), potassium nitrite (10 mM) or sodium L-glutamate (5 mM) were used as nitrogen sources. For aerobic batch culture, 50 ml volumes were rotated at 250 rpm in 250 ml flasks. During anaerobic growth, nitrate (30 mM) or nitrite also acted as the respective terminal electron acceptors for cellular respiration. The *Escherichia coli* strains were cultured aerobically on LB medium at 37 ^{o}C. Cell growth was followed by measuring the optical density (O.D.) of cultures at 600 nm. Antibiotics were used at the following final concentrations (μg·ml^{-1}): ampicillin (Ap), 100; kanamycin (Km), 25; rifampicin (Rif), 100; spectinomycin (Spec), 25; streptomycin (Sm), 60; tetracycline (Tc), 10; gentamycin (Gm), 20; chloramphenicol (Cm), 50. Where shown in the manuscript Figs bacterial growth curves are presented as arithmetic plots to minimise distortion of small changes in biomass during the early stages of the growth curve. For determination of growth rates, curves were analysed as semi-log plots from which the apparent maximum growth rate, $\mu_{max(app)}$ was determined from the gradient of the exponential growth phase.

Analytical methods

For preparation of subcellular fractions, *P. denitrificans* strains were cultured in mineral salts medium with nitrate and glutamate in a BioFlo IV fermenter (New Brunswick Scientific, USA) that was maintained at 30 ^{o}C, pH 7.2 with dissolved O_2 > 95%. Upon reaching an O.D.$_{600}$ value of approx. 0.6, a 10 litre culture volume was harvested and cells and fractionated to prepare cytoplasmic fractions (supplementary information). Assimilatory nitrate or nitrite reductase activity was assayed spectrophotometrically at pH 7.5 in the presence of the following electron donors: NADH (100 μM), NAD(P)H (100 μM) or dithionite-reduced Methyl Viologen (MV) at 1 mM. Activity assays were performed in quartz cuvettes of 1 cm path length. The reactions were followed by measuring the decrease in absorbance observed over time at 340 nm for NADH (or NADPH) dependent oxidation rates, or at 600 nm when monitoring re-oxidation of the reduced viologen cation radical [22]. Experiments were initiated by addition of $NaNO_3$ and $NaNO_2$, as required. NADH dependent assays performed on cytoplasmic cell fractions showed a constant background oxidation that was proportional to the amount of extract used. This rate was unaffected when experiments were performed under strict anaerobic conditions and addition of NAD^+ up to approx. 1 mM did not affect the rate of NADH-dependent nitrate or nitrite reduction. MV dependent rates were obtained under strict anaerobic conditions, using stock solutions of sodium nitrite and dithionite prepared and

stored anaerobically at 4 °C prior to use [15]. The following molar extinction coefficients, $\varepsilon_{340\ nm}$ = 6.22 x 10^3 $M^{-1}\cdot cm^{-1}$ (NADH) and $\varepsilon_{600\ nm}$ = 13.7 x 10^3 $M^{-1}\cdot cm^{-1}$ (MV) were used to calculate specific activities. Extracellular nitrate concentration was determined using a Dionex ICS-900 HPLC system fitted with a DS5 conductivity detector and AS40 automated sampler. Samples were diluted into analytical reagent grade water (Fisher Scientific, total N <0.1 ppm) and passed through a 0.2 µm syringe filter prior to injection onto a 2 x 250 mm IonPac® AS22 analytical carbonate eluent anion-exchange column. Nitrite concentration present in the extracellular medium was determined colourmetrically as described by Nicholas and Nason [23]. For separation of nitrate and nitrite reductase activities by anion-exchange chromatography a DEAE-Sepharose™ (GE Healthcare) column matrix was equilibrated in 5 mM L-ascorbate, 5mM EDTA, 50 mM Tris-HCl, pH 7.5. The column was loaded with cytoplasmic extract (obtained from *P. denitrificans* WT cells grown with nitrate as sole N-source), washed with 2 column volumes and then developed with a linear gradient of 0-0.5 M NaCl, over 1 column volume, at 1.5 $ml\cdot min^{-1}$ flow rate.

Samples for two-dimensional polyacrylamide gel electrophoresis (2D-PAGE) were prepared from *P. denitrificans* WT cells that were washed twice with 50 mM Tris-HCl (pH 8.0) and re-suspended in 10 mM Tris-HCl (pH 9.0) buffer solution containing DNaseI, RNaseA and protease inhibitors prior to lysis by sonication. Unbroken cells and cellular debris were removed by centrifugation (14000 x *g*) for 20 minutes at 4 °C. Supernatants were then subject to ultracentrifugation (40000 x *g*) for 1 hour at 4 °C to obtain soluble protein extracts. Protein was quantified using a 2-D Quant kit (GE Healthcare) according to the manufacturer's instructions and precipitated in 10% (w/v) trichloroacetic acid solution by incubation on ice for 2 hours, followed by centrifugation (14000 x *g*) for 20 minutes. Protein pellets were washed twice in the following solutions: 50 mM Tris-HCl (pH 8.0), 50 mM Tris (pH unadjusted) and 80% (v/v) ice-cold acetone. Final re-suspension was in 800 µl of solubilisation buffer that contained 7 M urea, 2 M thiourea, 4% (w/v) 3-[(3-cholamidopropyl)dimethylammonio]propane-1-sulphonic acid (CHAPS), 1% (w/v) Dithiothreitol (DTT), 1.5% (v/v) IPG buffer (pH range 4-7, GE Healthcare) and a trace of bromophenol blue. This mixture was vortexed for 2 hours and centrifuged (14000 x *g*) for 30 minutes after which the supernatant was recovered for use. Immobiline DryStrips (11 cm in length, pH range 4-7 from GE Healthcare) were rehydrated with 350 µg of protein for 12 hours into IPTG strip holders (GE Healthcare). Isoelectric focusing (IEF) of samples was then performed in an IPGphor ceramic manifold, covered with Plusone DryStrip cover fluid. Sample strips were focused for 20000 Volt hours in an IPGphor isoelectric focusing system (GE Healthcare). Following IEF, strips were equilibrated as previously described [24] and applied to 12.5% polyacrylamide gels performed with 30% acrylamide/bis solution, 37.5:1 or 29:1 ratio (Bio-Rad). Second dimension separation was performed by using the system Hoefer SE600 (GE Healthcare) and protein spots were visualised using Coomassie staining (2 $g\cdot l^{-1}$ Coomassie Brilliant Blue G250 and 0.5 $g\cdot l^{-1}$ R250 in 5% methanol, 42.5% ethanol and 10% glacial acetic acid). Triplicate 2D-PAGE separations were generated for each sample condition and gels were imaged using the GS-800 calibrated densitometer (Bio-Rad).

Protein identification was performed in the UCO-SCAI proteomics facility (University of Córdoba, Córdoba, Spain), a member of ProteoRed network. Protein spots of interest were excised automatically in a ProPic station (Genomic Solutions) and subjected to automated digestion with trypsin according to standard protocols in a ProGest station (Genomic Solutions). Peptide fragments were analyzed in a 4700 Proteomics Analyzer MALDI-TOF/TOF mass spectrometer (Applied Biosystems) with an accelerating voltage of 20 kV, in the m/z range 800 to 4000 (reflectron mode and delayed extraction were enabled, the elapse time was 120 nanoseconds). Proteins were identified by peptide mass fingerprinting and confirmed by MS/MS analysis of the 3 most abundant peptide ions. The MASCOT search engine (Matrixscience) was used for protein identification over the non-redundant National Center for Biotechnology Information (NCBI) database of proteins. The confidence in the peptide mass fingerprinting matches ($p < 0.05$) was based on the Molecular weight

Biochemical Journal Immediate Publication. Published on 24 Feb 2011 as manuscript BJ20101920

search method (MOWSE) score (higher than 65) and C.I. > 99.8%, and confirmed by the accurate overlapping of the matched peptides with major peaks present in the mass spectrum.

The detailed methodologies for cell fractionation and the construction and complementation of the *nas* mutants is described in the Supplementary Material.

RESULTS

Nitrate and nitrite as nitrogen sources for assimilation by *P. denitrificans*

In the absence of ammonium, *P. denitrificans* 1222 was able to grow aerobically using nitrate (Fig. 2A) or nitrite (Fig. 3A) as the sole N-source with values for $\mu_{max(app)}$ of 0.27 and 0.23 (± 0.01) h^{-1}, respectively at pH 7.2 (Table S2). Approximately 10 mM of nitrate or nitrite was consumed during batch culture with 50 mM succinate present as carbon substrate (Fig.s 2B and 3B). A maximum O.D. value of 2.15 (± 0.05) was reached after approx. 16 h, corresponding to a growth yield of ~100 mg dry wt cells·mM N^{-1} which were comparable to those obtained from cultures assimilating nitrogen from ammonium under carbon-sufficient growth conditions. With nitrate as sole N-source, a transient accumulation of ~1 mM nitrite in the extracellular medium was observed during growth (Fig. 2C). To probe the biochemical basis of this growth physiology, spectrophotometric solution assays were performed on subcellular fractions from *P. denitrificans* using reduced pyridine nucleotides as electron donor and either nitrate or nitrite as electron acceptor. Cytoplasmic fractions prepared from cells cultured with nitrate present as the sole N-source showed clear nitrate and nitrite dependent NADH-oxidation rates (Fig. 4). These activities were not detected in either periplasmic or membrane fractions prepared from the same cell cultures, or in any cell fraction when NADPH was used in place of NADH as electron donor. In addition, no activity above a stable background non-specific oxidation rate, which was proportional to the amount of cell extract used, was detected in cytoplasmic fractions from *P. denitrificans* cells when ammonium was the sole N-source (Fig. 4). This pattern of activity is consistent with the regulation of other bacterial *nas* systems that are subject to ammonium repression and nitrate induction [2, 5, 19, 31].

Analysis of the *P. denitrificans* genome (http://genome.jgi-psf.org/ parde/parde.home.html) reveals the presence of three gene clusters that likely code for different nitrate reductase systems. The genes for the respiratory systems Nar and Nap are located on chromosome 2 (NC_008687) and plasmid 1 (NC_008688), respectively. These clusters have been characterised previously in the closely related organism *Paracoccus pantotrophus* [12, 16, 32, 33]. In *P. denitrificans*, a third putative nitrate reductase gene is present within a cluster on chromosome 2 that is predicted to encode both the regulatory and structural elements for a cytoplasmic nitrate and nitrite reductase system (Pden_4455-4449). This gene cluster comprises seven open reading frames, *nasTSABGHC* (from 5' to 3') and spans some 10 kilobases from base pairs 1,657,840 to 1,667,370. A non-coding region of approx. 200 bases divides this cluster into two distinct functional units (Fig. 1A). The larger coding region, i.e., *nasABGHC,* which is the focus of this study, codes for putative redox proteins and substrate transport proteins and lies downstream of two genes encoding a putative nitrate and nitrite responsive two-component regulatory system, *nasT* and *nasS* [5]. The role *nasABGHC* in the assimilation of nitrogen from nitrate was confirmed by insertion of a kanamycin a resistance marker into the *nasA* gene (*nasA*Δ::Km*). Here, the configuration of the resistance cassette was selected such that transcriptional terminators were present to cause polar effect and prevent expression of all genes collectively transcribed downstream of *nasA*. Significantly, the *nasA*Δ::Km* mutant lost the capacity of the wild-type (WT) organism for aerobic growth with both nitrate and nitrite and thus established the importance of the *nasABGHC* region in the assimilation of both N-sources.

Biochemical properties of cytoplasmic NADH-dependent assimilatory nitrate and nitrite reduction

Spectrophotometric assays were performed to define the kinetic properties of the NADH-dependent nitrate reductase and nitrite reductase activities present in cytoplasmic fractions of *P. denitrificans*. Activity was measured as the concentration of NADH was varied at fixed saturating concentrations of nitrate or nitrite (Fig. 5A, outlined symbols), and conversely as the concentration of nitrate or nitrite was varied at fixed saturating NADH (Fig. 5A, solid symbols). In all cases, enzyme activity varied in accordance with the Michaelis-Menten description and Hanes analysis was performed to define kinetic constants for nitrate (Fig. 5B) and nitrite (Fig. 5C) reduction. Values for V_{max} of 111 and 302 (± 12) nmol·min^{-1}·mg protein^{-1} were determined for NADH oxidation with nitrate and nitrite present as electron acceptor, respectively. The V_{max} expressed as a function of NADH consumed for the nitrite reductase reaction was ~3-fold higher than that for the nitrate reductase reaction. However, when the electron stoichiometries of each reaction are taken into account, i.e., $2e^-/NO_3^-$ and $6e^-/NO_2^-$, the rates of nitrate and nitrite reduction are evenly matched, which would minimise the accumulation of toxic nitrite in the cytoplasm. The values of the Michaelis constant (K_M) for the reduction of nitrate and nitrite were 17 (± 4) and 5 (± 2) μM, respectively. By contrast K_M values determined for NADH-oxidation during the nitrate reductase or nitrite reductase reactions were in good agreement, at 51 (± 6) and 58 (± 8) μM respectively.

The elution of nitrate and nitrite reductase activities was monitored when a cytoplasmic fraction was subject to anion-exchange chromatography. Column fractions were assayed for nitrate and nitrite reductase activity using the non-physiological electron donor reduced Methyl Viologen (MV), which has been shown to donate electrons to both nitrate and nitrite reductases (either directly to the active sites or via electron transferring iron sulphur centres [14, 15, 34]). The two activities did not co-elute, with a large peak of MV-dependent nitrate reductase activity eluting at approx. 0.2 M NaCl, and the major peak of MV-dependent nitrite reductase activity eluting at higher approx. 0.3 M NaCl (Fig. 6A). Significantly, the nitrite reductase peak retained NADH-dependent nitrite reductase activity, but the nitrate reductase peak did not (Fig. 6B). A small protein population, eluting at approx. 0.28 M salt, retained both NADH-dependent and MV-dependent nitrate and nitrite reductase activities.

Genetic basis for a composite NADH-linked NasBGC nitrate and nitrite reductase system

Analysis of the *P. denitrificans* NasC primary amino acid sequence suggests that it binds an N-terminal [4Fe-4S] cluster and a molybdenum containing cofactor and so shares a similar general organisation to the assimilatory nitrate reductase of cyanobacteria (NarB) and the catalytic unit of the structurally-defined respiratory periplasmic nitrate reductases (NapA) [35-37]. It is also predicted to contain an additional C-terminal region of ~200 residues that may bind a [2Fe-2S] cluster, as also proposed for the nitrate reductase from *K. oxytoca* (NasA) [2, 31, 38, 39] (Fig. S1). Significantly, none of these nitrate reductases has a canonical NADH binding domain. A *P. denitrificans* strain mutated in *nasC* lost the capacity for aerobic growth with nitrate as N-source ($\mu_{max(app)}$ < 0.01 h^{-1}, maximum O.D. < 0.05), but retained the ability to grow using nitrite and displayed similar growth kinetics to WT ($\mu_{max(app)}$ = 0.23 ± 0.02 h^{-1}, maximum O.D. of 1.21 ± 0.05 was reached after approx. 16 h) (Fig. 7A and Table S2). This finding is consistent with NasC being the sole assimilatory nitrate reductase present during aerobic growth, reducing nitrate to nitrite, but playing no further role in the subsequent reduction of nitrite to ammonium. The *nasC* mutant could be grown in the presence of glutamate and nitrate ($\mu_{max(app)}$ = 0.25 ± 0.02, O.D.$_{max}$ = 1.3 ± 0.1). Under these conditions, cytoplasmic fractions from WT cells display both MV- and NADH-dependent nitrate reductase activities, but both activities were absent in the *nasC* mutant (Table 2).

In order for the assimilation of nitrogen from nitrate to proceed, the cytoplasmic nitrite generated by NasC must be further reduced to ammonium. NasB shares significant sequence homology to flavin, Fe-S, sirohaem-containing nitrite reductases [2, 11, 40] (Fig. S2). The *P. denitrificans* NasB polypeptide is predicted to contain N-terminal FAD and NADH binding domains, while highly conserved central and C-terminal sequence regions contain the cysteine residues

required for iron-sulphur cluster coordination and the nitrite/sulphite reductase ferredoxin half-domain associated with sirohaem binding (Fig. S2). A *P. denitrificans nasB* mutant was unable to grow aerobically with either nitrite or nitrate as sole N-source. In order to confirm that these growth defects were not caused by a downstream effect of the gene disruption process, the *nasB* strain was complemented with a pEG276-*nasB* expression construct. The presence of this plasmid allowed the *nasB* mutant to grow to near WT levels with either nitrate or nitrite as sole N-source, see Table S2 ($\mu_{max(app)}$ = 0.20 ± 0.02 h^{-1}, maximum O.D. = 1.23 ± 0.05). However, in the absence of the pEG276-*nasB* expression construct, no growth of the *nasB* mutant was observed, despite prolonged incubation for several days. This observation excludes the possibility of growth recovery through spontaneous mutation that may up-regulate a cryptic nitrite reductase. Cytoplasmic fractions obtained from the *nasB* mutant, grown in the presence of glutamate and nitrate, were assayed for NADH-dependent nitrate reductase and nitrite reductase activity. By contrast to that observed for WT cytoplasmic fractions, nitrite reductase activity was not detected in this mutant, consistent with the loss of the assimilatory nitrate reductase, NasB (Table 2). Significantly, nitrate reductase activity was also absent with NADH present as electron donor. Analysis of the NasC primary structure suggests that it lacks the NADH and FAD binding domains present in NasB that would be required for self-contained coupling of NADH oxidation to nitrate reduction (Figs S1 and S2). Therefore the absence of NADH-dependent nitrate reduction in the *nasB* mutant suggests a model in which the NADH-dehydrogenase domain of NasB provides electrons for both nitrite reduction by the sirohaem domain of NasB and nitrate reduction by NasC (Fig. 1B). Such a model is consistent with the similar K_M values for NADH observed with nitrate or nitrite in cytoplasmic extracts, and also the loss of NADH-nitrate reductase activity when nitrate reductase is separated from nitrite reductase by anion-exchange chromatography. Further evidence in support of this model was forthcoming from measuring nitrate reductase activity in the NasB mutant using the artificial electron donor MV, which can donate electrons directly to the nitrate reductase. Significantly, MV-dependent nitrate reductase activity was detected in the *nasB* mutant, which confirmed the presence of functional NasC that is unable to couple to NADH oxidation in the absence of NasB.

If the NADH-binding domain of NasB also serves NasC, then this raises the question of how electron transfer between NasB and NasC might occur. NasG is a strong candidate for mediating such electron transfer since it is predicted to be a Rieske-type iron-sulphur protein in which all residues (2 cysteine and 2 histidine) essential for coordination of a [2Fe-2S] redox site are conserved (Fig. S3). A *nasG* mutant was unable to grow with either nitrate or nitrite as sole N-source, under aerobic conditions. Expression of *nasG* in *trans* from a pEG276-*nasG* expression construct complemented the growth deficiencies of the *nasG* strain observed with nitrate and nitrite ($\mu_{max(app)}$ = 0.22 ± 0.07 h^{-1}, maximum O.D. = 1.31 ± 0.05), confirming specific disruption of *nasG* with no downstream effects, see Table S2. Unlike NasC and NasB there is no direct enzymatic assay with which to establish the synthesis of NasG. However, two-dimensional polyacrylamide gel electrophoresis (2D-PAGE) of soluble extracts from *P. denitrificans* WT, grown aerobically in the presence of glutamate and nitrate, revealed a protein with the mass and charge characteristics (12.1 kDa and pI of 5.6) of NasG that was absent in the *nasG* mutant (Fig. 8). Analysis by mass spectrometry confirmed that this spot was the NasG polypeptide (MASCOT Protein Score = 314; Table S3). Cytoplasmic fractions prepared from cells of the *nasG* mutant grown with glutamate and nitrate were devoid of NADH-dependent nitrate reductase or nitrite reductase activities, but MV-dependent activities were detected (Table 2). These findings confirm that NasG is essential for both NADH-dependent nitrate and nitrite reduction, consistent with the protein mediating electron transfer from NADH to the active sites of both NasB and NasC (Fig. 1B). It was also notable that the MV-dependent nitrite reductase activity was unstable with a half-life of approx. 50 minutes following preparation of the cytoplasmic extract. This instability was reflected in 2D-PAGE analysis of the WT and *nasG* strains. In WT extract a triad of protein spots of ~88 kDa and PI of ~5.6 were each established by mass spectrometry to be NasB (MASCOT Protein Score = 622; Table S3) (Fig. 8A). As

expected this triad was absent in the *nasB* mutant. However, they could also not be identified in extracts from the NasG mutant despite analysis of a number of samples at different protein loadings. By contrast the NasG spot could be detected at ~WT levels in 2D-PAGE analysis of the *nasB* strain (Fig. 8). Thus NasG is stable in the absence of NasB, but may be required for NasB stability. It was notable that in the *nasB* strain a new protein spot was very prominent in cells grown with nitrate and glutamate. This spot was identified by mass spectrometry to be a member of the Hsp20 family of chaperones that protect unfolded proteins from aggregation (MASCOT Protein Score = 632; Table S3) [41]. This response may reflect the need to protect NasG whilst it is being assembled in the absence of its NasB partner or a response to protein damage by nitrosative stress arising from a lesion in cytoplasmic nitrite reduction.

The contribution of NasA and NasH to nitrate and nitrite transport

Delivery of nitrate and nitrite from the external environment to the cytoplasmic NasBGC system requires that the two N-oxyanions are transported across the cytoplasmic membrane against a membrane potential that is negative on the inside of the membrane. NasA and NasH are good candidate transporters for facilitating assimilatory N-oxyanion import. NasA is predicted to be a 12 trans-membrane helix transporter of the major facilitator super-family (MFS), see Fig.s 1B and S4. *P. denitrificans* synthesizes another well characterised MFS family member in the presence of nitrate under anoxic conditions, NarK that serves to transport nitrate for the respiratory nitrate reductase system, NarGHI [16, 17, 33] (Fig. 1B). A non-polar *nasA* strain was constructed and was found to be strongly attenuated for aerobic growth with nitrate as sole N-source ($\mu_{max(app)}$ = 0.04 ± 0.01 h^{-1}, maximum O.D. = 0.38 ± 0.05), demonstrating that NasA is the major nitrate transporter under these growth conditions (Fig. 2A and Table S2). Despite disruption of the *nasA* gene this strain retained the ability to grow aerobically with nitrite as sole N-source albeit with slower growth ($\mu_{max(app)}$ = 0.20 ± 0.01 h^{-1}, maximum O.D. = 1.99 ± 0.05) and nitrite consumption kinetics than that observed for WT cells, implying that NasA may make a contribution to, but is not essential for, nitrite uptake into the cell (Fig. 3 and Table S2). Efforts to complement the *nasA* strain using the same complementation vector system used successfully for *nasB* and *nasG* was unsuccessful, possibly due to a failure to assemble the integral membrane protein. However, evidence that there were no polar effects of the *nasA* mutation on downstream gene expression is given by the detection of NADH-dependent nitrate (~10 nmoles·min^{-1}·mg $protein^{-1}$) and nitrite (~30 nmoles·min^{-1}·mg $protein^{-1}$) reductase activity at WT levels in cells grown on glutamate-nitrate medium, which would require transcription of *nasBGC*, which lies downstream of *nasA*.

NasH is a putative member of the formate-nitrite transporter super-family that includes NirC from *E. coli* (Fig. S5) [42-44]. Recent evidence suggests that NirC can move nitrite *bi*-directionally across the cytoplasmic membrane during anaerobic growth of *E. coli* (29). NasH is thus a prime candidate for mediating nitrite uptake or export and so may be important for nitrite homeostasis during nitrate assimilation. Perhaps surprisingly though, the *P. denitrificans nasH* mutant displayed similar growth kinetics and yields ($\mu_{max(app)}$ = 0.28 ± 0.01 h^{-1}, maximum O.D. = 1.79 ± 0.09) to that observed for WT, when cultured aerobically with either nitrate or nitrite as sole N-source at pH 7.2 (Fig.s 2 and 3). The pattern of nitrite consumption from the extracellular medium during growth with nitrite as sole N-source was also similar in the WT and *nasH* strains (Fig. 3B), as was the transient accumulation of approx. 1 mM nitrite observed during the mid to late exponential growth phase when nitrate was present as sole N-source (Fig. 2C). A double *nasA nasH* mutant also retained the ability to grow with nitrite as sole N-source, at pH 7.2 ($\mu_{max(app)}$ = 0.20 ± 0.01 h^{-1}, maximum O.D. = 1.72 ± 0.05), displaying similar growth kinetics to the *nasA* strain (Fig. 3A and Table S2). Nitrite is a protonatable anion that exists in equilibrium with nitrous acid ($NO_2^- + H^+ \leftrightarrow HNO_2$), with a p$K_a$ value of 3.3 [17]. Thus, at pH 7 with an external nitrite concentration of 10 mM, the concentration of HNO_2 is present in the low micromolar range. This acid could freely diffuse across the phospholipid bilayer, dissociate in the cytoplasm, and so deliver nitrite to the NasBGC complex without recourse to a

specific nitrite uptake system. The extent to which this could occur will be decreased at higher pH. It was therefore notable that when the *nasH* and *nasA nasH* mutants were grown at pH 9.2 with nitrite as the sole N-source, significant attenuation in growth and nitrite consumption was observed in both cases, thus demonstrating a role for NasH in nitrite import (Figs 3C, 3D and Table S2).

Functional substitution of Nar components for Nas components in anaerobic nitrate assimilation

P. denitrificans could grow anaerobically, as well as aerobically, with nitrate or nitrite as the sole N-source (Fig. 7 and Table S2). Under these growth conditions energy conservation is via nitrate and nitrite respiration through the anaerobically synthesised Nar and Nir systems, respectively [12]. The Nar system includes the respiratory ubiquinol/nitrate oxidoreductase, NarGHI of which the NarG nitrate-reductase subunit is located at the cytoplasmic face of the cytoplasmic membrane and a fusion protein of two NarK-type modules facilitates nitrate and nitrite movement across the membrane (Fig. 1B). To investigate whether the NarG and NarK proteins could functionally substitute for NasC and NasA, the *nas* mutants were cultured under anaerobic conditions with nitrate present as sole N-source and electron acceptor anoxic, conditions that result in *nar* gene expression. Both the *nasA* and *nasC* mutants showed significant growth under these conditions (Fig. 7B), despite being unable to grow aerobically with nitrate as sole N-source (compare Figs 2A and 7B). The *nasC* mutant was also able to grow anaerobically with nitrite present as both sole N-source and respiratory electron acceptor (Fig. 7C). Unlike the *nasC* strain, however, neither the *nasB* or *nasG* mutants retained the ability to grow anaerobically with nitrate or nitrite, demonstrating that the NADH-dependent NasBG nitrite reductase was indispensible to both oxic and anoxic assimilation of nitrate and nitrite.

DISCUSSION

This work has established that *P. denitrificans* NasC and NasB are both part of a cytoplasmic NADH-dependent assimilatory nitrate and nitrite reduction system. However, analysis of the primary structures of both proteins revealed that only NasB has a canonical FAD-dependent NADH binding domain. A bioinformatic analysis of predicted gene products for *nasC* and *nasB* homologues from the diverse bacterial phyla suggests that this is a common feature (Fig. S6). There is no bacterial assimilatory nitrate reductase that we can identify that has an NADH binding site. As such, this makes them quite distinct from plant and fungal assimilatory nitrate reductases in which NAD(P)H binding domains are ubiquitous [45]. In the present study we have reported genetic and biochemical data that suggests that the NADH-oxidising FAD domain of NasB provides electrons for both nitrite reduction by the NasB ferredoxin:sirohaem active site and nitrate reduction by the NasC molybdenum cofactor active site: (i) NADH-dependent nitrate reductase activity is lost when the nitrate reductase is separated from the NADH-dependent nitrite reductase; (ii) the K_M value for NADH determined with either nitrate or nitrite is the same in cytoplasmic fractions from WT cells; (iii) non-polar deletion of *nasB* results in loss of aerobic growth with nitrate as sole N-source; (iv) non-polar deletion of *nasB* results in loss of NADH-dependent nitrate reductase activity, but not MV-dependent nitrate reductase activity. We also show that the putative Rieske [2Fe-2S] ferredoxin, NasG is required for these NADH-dependent electron transfer processes because in a *nasG* strain: (i) no growth is observed with either nitrate or nitrite as sole N-source and (ii) NADH-dependent nitrate and nitrate reductase activities are absent in cytoplasmic extracts, but MV-dependent activities are detected. These findings imply that NasG can interact in the cytoplasm with both NasB and NasC, and lead us to propose a model in which it serves at the interface of a composite NADH-dependent nitrate and nitrite reductase system, NasBGC (Fig. 1B).

It is notable that many bacterial *nas* clusters that we have examined encode a NasG-like protein, in addition to an NADH-oxidising sirohaem-dependent nitrite reductase, suggesting an important conserved function (Fig. S6). It is absent in the *Synechococcus elongatus* cluster (Fig. 9),

but in this case the photoautotroph uses reduced ferredoxin generated from photosystem I to drive nitrate and nitrite reduction [19]. A *nasG* homologue is also absent from the *nas* cluster of *Klebsiella* species (Fig. S6) [39]. However, these novel larger NasB proteins show an extended C-terminal region of approx. 100 residues that shares homology with NasG. In addition, in *Klebsiella oxytoca* there is a gene in the *nas* operon that codes for a flavoprotein which may substitute for NasG or support it in enabling electron transfer from NADH to the nitrate reductase subunit. A homologue of this gene may also be playing such a role in *Bacillus subtilis* [4], whilst in *Klebsiella pneumoniae* this gene appears to be fused to the gene for the nitrite reductase (Fig. S6). Nevertheless, even taking these exceptions into account, the widespread distribution of NasG-type modules leads us to propose that the composite NasBGC system exemplified here by *P. denitrificans* is a very common feature of Nas systems in phylogenetically diverse bacteria. Though the interaction between NasC and NasBG does not resist anion-exchange chromatography, there is precedent for a stable interaction between a molybdenum cofactor dependent enzyme and Rieske-type ferredoxin. Intriguingly, the catalytic subunit of the arsenite oxidase from *Alcaligenes faecalis* forms a stable heterodimeric complex and co-crystallises with its redox partner, a Reiske-type [2Fe-2S] protein that shares sequence similarity with NasG (~40 %) [46, 47]. Structural studies also revealed that the iron-sulphur centres present in each subunit are ideally situated, at <14 Å (edge-to-edge) from one another across the heterodimeric interface, to facilitate rapid electron transfer that does not limit catalysis [47]. Thus, the NasC-NasG interaction may be a weaker manifestation of the protein-protein interaction observed in the arsenite oxidase complex. The genetic evidence that NasG is a dedicated ferredoxin for the NasBC system and that the NasB protein is possibly unstable is perhaps surprising given that *P. denitrificans* genome predicted to encode a number of small cytoplasmic ferredoxins. However, precedent for this may be found in the *E. coli* cytoplasmic nitrite reductase system. *E. coli* is unable to grow aerobically with nitrite as sole N-source, but when grown under nitrate-rich anoxic conditions a respiratory nitrate reductase NarG and a sirohaem:ferredoxin-type nitrite reductase, NirB operate in the cytoplasm to respire nitrate and detoxify the nitrite product (Fig. S6) [50]. *E. coli* can also grow anaerobically with nitrite as sole N-source under conditions where the *nirB* gene encoding this anaerobically-inducible nitrite reductase is expressed [50, 51]. *E. coli nirB* is a homologue of *P. denitrificans nasB* (65% similarity) and both genes are found upstream of their ferredoxin partners, *E. coli nirD* and *P. denitrificans nasG*, respectively, which share 59% similarity (Fig. S6). Significantly, like the *P. denitrificans nasG* mutant, NADH-dependent nitrite reductase activity is also lost in an *E. coli nirD* mutant [52]. In both *E. coli* and *P. denitrificans* the *nirB*/*nasB* and *nirD*/*nasG* loci lie immediately upstream of a gene encoding a transporter *nirC*/*nasH* (55% similarity) in their respective genomes (Fig. S6). Here, by growing *P. denitrificans* at high pH to minimise HNO_2 formation, we have shown that *nasH* contributes to nitrite uptake. These observations show a clear genetic and biochemical link between two nitrite reductase systems with distinct primary functions in nitrite assimilation and detoxification.

Turning finally to the rescue of *nasA* and *nasC* mutants under anaerobic growth conditions by the respiratory Nar system. This is consistent with functional overlap between two physiologically distinct systems whose cellular function commonly requires the import and cytoplasmic based reduction of nitrate. In this respect, it is notable that an assimilatory nitrate reductase gene is absent from some assimilatory gene clusters in nitrate-assimilating bacteria where the respiratory nitrate reductase *narG* gene is present at a different genetic locus in the bacterium. A noteworthy example is *Mycobacterium* (Fig. S6), in which *narG* mutants cannot grow with nitrate as sole N-source [48, 49]. The interchangeability between NasC and NarGHI in anaerobic assimilatiory nitrate reduction is also consistent with the dissociation of NasC from NasBG observed during anion-exchange chromatography, suggesting a modular arrangement in which NasBG can exist as a stable functional entity in the absence of NasC.

ACKNOWLEDGEMENTS

This work was supported by the Biotechnology and Biological Sciences Research Council [grant numbers BBE0219991 and BBD5230191]. DJR is a Royal Society and Wolfson Foundation for Merit Award Fellow. MDR thanks the Ministerio de Ciencia y Tecnología for supporting the work through Grants BIO2005-07741-C02-01 and BIO2008-04542-C02-01 and the Junta de Andalucía for Grant CVI1728. VML-A was recipient of a postdoctoral fellowship from the Ministerio de Ciencia y Tecnología, Spain. We thank Dr Niels-Ulrik Frigaard (University of Copenhagen, Denmark) for providing the pSRA2 plasmid containing the streptomycin and spectinomycin resistance cassette and Dr Eva Pérez Reinado (University of Cordoba, Spain) for the mobilizable vector pSUP202*. We are also grateful to the U.S. Department of Energy for providing the funds to sequence the genome of *Paracoccus denitrificans* PD1222.

REFERENCES

1 Van 'T Riet, J., Stouthamer, A. H. and Planta, R. J. (1968) Regulation of nitrate assimilation and nitrate respiration in *Aerobacter aerogenes*. J. Bacteriol. **96**, 1455-1464

2 Lin, J. T. and Stewart, V. (1998) Nitrate assimilation by bacteria. Adv. Microb. Physiol. **39**, 1-30, 379

3 Pino, C., Olmo-Mira, F., Cabello, P., Martínez-Luque, M., Castillo, F., Roldán, M. D. and Moreno-Vivián, C. (2006) The assimilatory nitrate reduction system of the phototrophic bacterium *Rhodobacter capsulatus* E1F1. Biochem. Soc. Trans. **34**, 127-129

4 Ogawa, K., Akagawa, E., Yamane, K., Sun, Z. W., LaCelle, M., Zuber, P. and Nakano, M. M. (1995) The *nasB* operon and *nasA* gene are required for nitrate/nitrite assimilation in *Bacillus subtilis*. J. Bacteriol. **177**, 1409-1413

5 Gutierrez, J. C., Ramos, F., Ortner, L. and Tortolero, M. (1995) *nasST*, two genes involved in the induction of the assimilatory nitrite-nitrate reductase operon (*nasAB*) of *Azotobacter vinelandii*. Mol. Microbiol. **18**, 579-591

6 Moreno-Vivián, C. and Flores, E. (2007) Nitrate assimilation in bacteria, In Biology of the nitrogen cycle (Bothe, H., Ferguson, S. J. and Newton, W. E., eds.), Elsevier, Amsterdam, NL

7 Allen, A. E., Booth, M. G., Frischer, M. E., Verity, P. G., Zehr, J. P. and Zani, S. (2001) Diversity and detection of nitrate assimilation genes in marine bacteria. Appl. Environ. Microbiol. **67**, 5343-5348

8 Allen, A. E., Booth, M. G., Verity, P. G. and Frischer, M. E. (2005) Influence of nitrate availability on the distribution and abundance of heterotrophic bacterial nitrate assimilation genes in the Barents Sea during summer. Aquat. Microb. Ecol. **39**, 247-255

9 Cliff, J. B., Gaspar, D. J., Bottomley, P. J. and Myrold, D. D. (2002) Exploration of inorganic C and N assimilation by soil microbes with time-of-flight secondary ion mass spectrometry. Appl. Environ. Microbiol. **68**, 4067-4073

10 Kirchman, D. L. (2000) Microbial ecology of the oceans, John Wiley & Sons

11 Richardson, D. J., Berks, B. C., Russell, D. A., Spiro, S. and Taylor, C. J. (2001) Functional, biochemical and genetic diversity of prokaryotic nitrate reductases. Cell. Mol. Life Sci. **58**, 165-178

12 Berks, B. C., Ferguson, S. J., Moir, J. W. B. and Richardson, D. J. (1995) Enzymes and associated electron transport systems that catalyse the respiratory reduction of nitrogen oxides and oxyanions. Biochim. Biophys. Acta **1232**, 97-173

13 Richardson, D. J. and Ferguson, S. J. (1992) The influence of carbon substrate on the activity of the periplasmic nitrate reductase in aerobically grown *Thiosphaera pantotropha*. Arch. Microbiol. **157**, 535-537

14 Anderson, L. J., Richardson, D. J. and Butt, J. N. (2001) Catalytic protein film voltammetry from a respiratory nitrate reductase provides evidence for complex electrochemical modulation of enzyme activity. Biochemistry **40**, 11294-11307

15 Gates, A. J., Richardson, D. J. and Butt, J. N. (2008) Voltammetric characterization of the aerobic energy-dissipating nitrate reductase of *Paracoccus pantotrophus*: exploring the activity of a redox-balancing enzyme as a function of electrochemical potential. Biochem. J. **409**, 159-168

16 Wood, N. J., Alizadeh, T., Richardson, D. J., Ferguson, S. J. and Moir, J. W. (2002) Two domains of a dual-function NarK protein are required for nitrate uptake, the first step of denitrification in *Paracoccus pantotrophus*. Mol. Microbiol. **44**, 157-170

17 Goddard, A. D., Moir, J. W. B., Richardson, D. J. and Ferguson, S. J. (2008) Interdependence of two NarK domains in a fused nitrate/nitrite transporter. Mol. Microbiol. **70**, 667-681

18 Sears, H. J., Little, P. J., Richardson, D. J., Berks, B. C., Spiro, S. and Ferguson, S. J. (1997) Identification of an assimilatory nitrate reductase in mutants of *Paracoccus denitrificans* GB17 deficient in nitrate respiration. Arch. Microbiol. **167**, 61-66

19 Flores, E., Frías, J. E., Rubio, L. M. and Herrero, A. (2005) Photosynthetic nitrate assimilation in cyanobacteria. Photosynth. Res. **83**, 117-133

20 Robertson, L. A. and Kuenen, J. G. (1983) *Thiosphaera pantotropha* gen. nov. sp. nov., a facultatively anaerobic, facultatively autotrophic sulphur bacterium. J. Gen. Microbiol. **129**, 2847-2855

21 Robertson, L. A., van Niel, E. W. J., Torremans, R. A. M. and Kuenen, J. G. (1988) Simultaneous nitrification and denitrification in aerobic chemostat cultures of *Thiosphaera pantotropha*. Appl. Environ. Microbiol. **54**, 2812-2818

22 Michaelis, L. and Hill, E. S. (1933) The viologen indicators. J. Gen. Physiol. **16**, 859-873

23 Nicholas, D. J. D. and Nason, A. (1957) Determination of nitrite and nitrate. Methods Enzymol. **3**, 981-984

24 Luque-Almagro, V. M., Huertas, M. J., Roldán, M. D., Moreno-Vivián, C., Martínez-Luque, M., Blasco, R. and Castillo, F. (2007) The cyanotrophic bacterium *Pseudomonas pseudoalcaligenes* CECT5344 responds to cyanide by defence mechanisms against iron deprivation, oxidative damage and nitrogen stress. Environ. Microbiol. **9**, 1541-1549

25 Labes, M., Pühler, A. and Simon, R. (1990) A new family of RSF1010-derived expression and *lac*-fusion broad-host-range vectors for Gram-negative bacteria. Gene **89**, 37-46

26 Yanisch-Perron, C., Vierra, J. and Messing, J. (1985) Improved M13 phage cloning vectors and host strains: nucleotide sequences of the M13mp18 and pUC19 vectors. Gene **33**, 103-119

27 Frigaard, N. U., Li, H., Milks, K. J. and Bryant, D. A. (2004) Nine mutants of *Chlorobium tepidum* each unable to synthesize a different chlorosome protein still assemble functional chlorosomes. J. Bacteriol. **186**, 646–653

28 Simon, R., Priefer, U. and Pühler, A. (1983) A broad host range mobilization system for *in vivo* genetic engineering: transposon mutagenesis in Gram negative bacteria. Nat. Biotechnol. **1**, 784-791

29 Figurski, D. H. and Helinski, D. R. (1979) Replication of an origin-containing derivative of plasmid RK2 dependent on a plasmid function provided in *trans*. Proc. Natl. Acad. Sci. U.S.A. **76**, 1648–1652

30 Gordon, E. H., Sjögren, T., Löfqvist, M., Richter, C. D., Allen, J. W., Higham, C. W., Hajdu, J., Fülöp, V. and Ferguson, S. J. (2003) Structure and kinetic properties of *Paracoccus pantotrophus* cytochrome cd_1 nitrite reductase with the d_1 heme active site ligand tyrosine 25 replaced by serine. J. Biol. Chem. **278**, 11773–11781

31 Lin, J. T. and Stewart, V. (1996) Nitrate and nitrite-mediated transcription antitermination control of *nasF* (nitrate assimilation) operon expression in *Klebsiella pheumoniae* M5al. J. Mol. Biol. **256**, 423-435

32 Berks, B. C., Richardson, D. J., Reilly, A., Willis, A. C. and Ferguson, S. J. (1995) The *napEDABC* gene cluster encoding the periplasmic nitrate reductase system of *Thiosphaera pantotropha*. Biochem. J. **309**, 983-992

33 Wood, N. J., Alizadeh, T., Bennett, S., Pearce, J., Ferguson, S. J., Richardson, D. J. and Moir, J. W. B. (2001) Maximal expression of membrane-bound nitrate reductase in *Paracoccus* is induced by nitrate via a third FNR-like regulator named NarR. J. Bacteriol. **183**, 3606-3613

34 Vega, J. M. and Kamin, H. (1977) Spinach nitrite reductase. Purification and properties of a siroheme-containing iron-sulfur enzyme. J. Biol. Chem. **252**, 896-909

35 Jepson, B. J. N., Anderson, L. J., Rubio, L. M., Taylor, C. J., Butler, C. S., Flores, E., Herrero, A., Butt, J. N. and Richardson, D. J. (2004) Tuning a nitrate reductase for function. The first spectropotentiometric characterization of a bacterial assimilatory nitrate reductase reveals novel redox properties. J. Biol. Chem. **279**, 32212-32218

36 Jepson, B. J. N., Marietou, A., Mohan, S., Cole, J. A., Butler, C. S. and Richardson, D. J. (2006) Evolution of the soluble nitrate reductase: defining the monomeric periplasmic nitrate reductase subgroup. Biochem. Soc. Trans. **34**, 122-126

37 Jepson, B. J. N., Mohan, S., Clarke, T. A., Gates, A. J., Cole, J. A., Butler, C. S., Butt, J. N., Hemmings, A. M. and Richardson, D. J. (2007) Spectropotentiometric and structural analysis of the periplasmic nitrate reductase from *Escherichia coli*. J. Biol. Chem. **282**, 6425-6437

38 Lin, J. T., Goldman, B. S. and Stewart, V. (1993) Structures of genes *nasA* and *nasB*, encoding assimilatory nitrate and nitrite reductases in *Klebsiella pneumoniae* M5al. J. Bacteriol. **175**, 2370-2378

39 Lin, J. T., Goldman, B. S. and Stewart, V. (1994) The *nasFEDCBA* operon for nitrate and nitrite assimilation in *Klebsiella pneumoniae* M5al. J. Bacteriol. **176**, 2551-2559

40 Olmo-Mira, M. F., Cabello, P., Pino, C., Martínez-Luque, M., Richardson, D. J., Castillo, F., Roldán, M. D. and Moreno-Vivián, C. (2006) Expression and characterization of the assimilatory NADH-nitrite reductase from the phototrophic bacterium *Rhodobacter capsulatus* E1F1. Arch. Microbiol. **186**, 339-344

41 Narberhaus, F. (2002) α-Crystallin-type heat shock proteins: socializing minichaperones in the context of a multichaperone network. Microbiol. Mol. Biol. Rev. **66**, 64-93

42 Jia, W. and Cole, J. A. (2005) Nitrate and nitrite transport in *Escherichia coli*. Biochem. Soc. Trans. **33**, 159-161

43 Jia, W., Tovell, N., Clegg, S., Trimmer, M. and Cole, J. (2009) A single channel for nitrate uptake, nitrite export and nitrite uptake by *Escherichia coli* NarU and a role for NirC in nitrite export and uptake. Biochem. J. **417**, 297-304

44 Wang, Y., Huang, Y., Wang, J., Cheng, C., Huang, W., Lu, P., Xu, Y. N., Wang, P., Yan, N. and Shi, Y. (2009) Structure of the formate transporter FocA reveals a pentameric aquaporin-like channel. Nature **462**, 467-472

45 Campbell, W. H. (2001) Structure and function of eukaryotic NAD(P)H:nitrate reductase. Cell. Mol. Life Sci. **58**, 194-204

46 Anderson, G. L., Williams, J. and Hille, R. (1992) The purification and characterization of arsenite oxidase from *Alcaligenes faecalis*, a molybdenum-containing hydroxylase. J. Biol. Chem. **267**, 23674-23682

47 Ellis, P. J., Conrads, T., Hille, R. and Kuhn, P. (2001) Crystal structure of the 100 kDa arsenite oxidase from *Alcaligenes faecalis* in two crystal forms at 1.64 Å and 2.03 Å. Structure **9**, 125-132

48 Amon, J., Titgemeyer, F. and Burkovski, A. (2009) A genomic view on nitrogen metabolism and nitrogen control in mycobacteria. J. Mol. Microbiol. Biotechnol. **17**, 20-29

49 Malm, S., Tiffert, Y., Micklinghoff, J., Schultze, S., Joost, I., Weber, I., Horst, S., Ackermann, B., Schmidt, M., Wohlleben, W., Ehlers, S., Geffers, R., Reuther, J. and Bange, F. C. (2009) The roles of the nitrate reductase NarGHJI, the nitrite reductase NirBD and the response regulator GlnR in nitrate assimilation of *Mycobacterium tuberculosis*. Microbiology **155**, 1332-1339

50 Potter, L., Angove, H., Richardson, D. and Cole, J. (2001) Nitrate reduction in the periplasm of gram-negative bacteria. Adv. Microb. Physiol. **45**, 51-112

51 Cole, J. A., Coleman, K. J., Compton, B. E., Kavanagh, B. M. and Keevil, C. W. (1974) Nitrite and ammonia assimilation by anaerobic continuous cultures of *Escherichia coli*. J. Gen. Microbiol. **85**, 11-22

52 Harborne, N. R., Griffiths, L., Busby, S. J. and Cole, J. A. (1992) Transcriptional control, translation and function of the products of the five open reading frames of the *Escherichia coli* nir operon. Mol. Microbiol. **6**, 2805-2813

53 De Vries, G. E., Harms, N., Hoogendijk, J. and Stouthamer, A. H. (1989) Isolation and charactrization of *Paracoccus denitrificans* mutants with increased conjugation frequencies and pleiotropic loss of a (nGATCn) DNA-modifying property. Arch. Microbiol. **152**, 52-57

54 Sambrook, J., Fritsch, E. F. and Maniatis, T. (1989) Molecular cloning: a laboratory manual, Cold Spring Harbor Laboratory Press, New York

FIGURE LEGENDS

Fig. 1. Genetic and proposed functional organisation of the assimilatory nitrate reductase system from *P. denitrificans* PD1222. The *nas* gene cluster includes seven open reading frames, *nasTSABGHC* (A). The gene products have the following putative roles, two regulatory components (*nasS and nasT*), two nitrogen oxyanion transporters (*nasA* and *nasH*), nitrate and nitrite reductases (*nasC* and *nasB*, respectively) and a ferredoxin (*nasG*). Three distinct nitrate reductase systems are present in *P. denitrificans* (B). The periplasmic (NapABC) and membrane-bound (NarGHI) enzymes are ubiquinol-dependent respiratory nitrate reductases. NarK, a nitrate importer, moves nitrate into the cytoplasm and also exports nitrite, the product of nitrate reduction, to the periplasm to support respiratory denitrification. For assimilatory nitrate reduction, electrons likely derived from NADH within the FAD-containing nitrite reductase (NasB) flow to the nitrate reductase (NasC), possibly via the small ferredoxin (NasG). In the Nas system there are two transporters, NasA and NasH, which are predicted to be involved in nitrate and nitrite transport, respectively. Note that there is no common nomenclature for assimilatory nitrate and nitrite reductase genes in prokaryotes. In the case of nitrite reductase genes the '*nir*' prefix is quite widely used, but since *P. denitrificans* has a separate respiratory nitrite reductase '*nir*' gene cluster, this term would be inappropriate. Likewise the '*nar*' prefix is sometimes used for the assimilatory nitrate reductase genes, but this would also be inappropriate for *P. denitrificans* which also has a *nar* gene cluster encoding the respiratory nitrate reductase system. Hence we have adopted the *nas* prefix for the genes encoding the assimilatory nitrate and nitrite reductase system of *P. denitrificans*. The term 'nH^+' indicates that the number of protons (n) moved across the membrane is not known.

Fig. 2. Aerobic growth of *P. denitrificans* WT (squares), *nasA* (circles), *nasH* (triangles) and *nasA nasH* (inverted triangles) strains with nitrate present as the sole nitrogen source (A). Extracellular nitrate (B) and nitrite (C) concentrations are shown for growth of strains described in (A). Data shown are the average of triplicate determinations.

Fig. 3. Aerobic growth of *P. denitrificans* WT (squares), *nasA* (circles), *nasH* (triangles) and *nasA nasH* (inverted triangles) strains with nitrite present as the sole nitrogen source. Cells were cultured at pH 7.2 (A) and pH 9.2 (C), during which extracellular nitrite concentration was determined (shown in B and C, respectively). Data shown are the average of triplicate determinations.

Fig. 4. The nitrate and nitrite reductase activity of cytoplasmic fractions of *P. denitrificans.* Fractions prepared from cells grown with either nitrate (solid lines) or ammonium (dashed lines) as sole nitrogen source were assayed for nitrate (A) and nitrate (B) reductase activity. Spectrophotometric assays were performed at pH 7.5 in the presence of NADH (100 µM). The reaction was initiated by addition of either nitrate or nitrite and followed by measuring the decrease in absorbance observed over time at 340 nm.

Fig. 5. Kinetic properties of NADH-dependent assimilatory nitrate and nitrite reduction. NADH dependent nitrate (squares) and nitrite (circles) reductase activities present in cytoplasmic fractions from *P. denitrificans* grown with nitrate as sole nitrogen source (A). Solid and outlined symbols show (i) NADH oxidation rates observed with substrate concentration varied against fixed NADH (200 µM), and (ii) NADH varied against fixed substrate concentration (200 µM), respectively. Hanes analysis of nitrate reductase (B) and nitrite reductase activities (C) presented in A. Values for K_M of 17 and 5 (± 2) µM were derived for nitrate and nitrite reduction, respectively. Similar K_M values for NADH of 58 and 51 (± 8) µM were determined with nitrate or nitrite as electron acceptor, respectively. From (i) V_{max} values for nitrate and nitrite reduction were 95 and 86 (± 10) units

respectively, and (ii) V_{max} values of 111 and 302 (± 12) units were determined for NADH oxidation with nitrite and nitrite, respectively (1 unit ≡ 1 nmol·min^{-1}·mg protein^{-1}).

Fig. 6. A representative activity-elution profile observed during anion exchange chromatography. Panels A and B show MV- and NADH-dependent nitrate (solid symbols) or nitrite (outlined symbols) reductase activities present in column fractions, respectively. DEAE-Sepharose™ column matrix was equilibrated in 5 mM L-ascorbate, 5mM EDTA, 50 mM Tris-HCl, pH 7.5. The column was loaded with a cytoplasmic extract from *P. denitrificans* grown with nitrate as sole nitrogen source, washed with 2 column volumes and then developed with a linear gradient of 0-0.5 M NaCl, over 1 column volume at 1.5 ml·min^{-1} flow rate.

Fig. 7. Growth curves for the *nasC* and *nasA* strains under aerobic and anaerobic conditions. Aerobic growth of the *nasC* strain with either nitrate (squares) or nitrite (circles) present as the sole nitrogen source (A). Anaerobic growth of WT (squares), *nasA* (circles) and *nasC* (triangles) strains with either nitrate (B) or nitrite (C) present as the sole nitrogen source. Data shown are the average of triplicate determinations.

Fig. 8. 2D-PAGE analysis of soluble extracts from *P. denitrificans*. 350 µg of protein was applied to 11 cm strips. Isoelectric focusing was performed in the range 4-7. The 12.5% polyacrylamide gels formed with either with 30% acrylamide/bis solution, 37.5:1 (A) or 29:1 ratio (B).

Table 1. Bacterial strains and plasmids used in this work.

Strain or plasmid	Relevant characteristics	Source or reference
Bacteria		
Paracoccus denitrificans		
wild-type, PD1222	Rif^r, Spec^r, enhanced conjugation frequencies	[53]
*nasA*Δ::*Km**	Km^r (polar mutation)	This work
*nasA*Δ::Km	Km^r	This work
*nasB*Δ::Sm	Sm^r	This work
*nasG*Δ::Sm	Sm^r	This work
*nasH*Δ::Sm	Sm^r	This work
*nasC*Δ::Tc	Tc^r	This work
*nasA*Δ::Km/*nasH*Δ::Sm	Km^r, Sm^r	This work
Escherichia coli		
DH5*α*	*supE*44 Δ*lac*U169 (ϕ80*lacZ*ΔM15) *hsdR*17 *recA*1 *endA*1 *gyrA*96 *thi*-1 *relA*1 plasmid host	[54]
pRK2013	Km^r, Tra$^+$ (pRK2013 encoded) helper strain	[29]
Plasmids		
pUC18	Ap^r, Lac$^+$, cloning vector	[26]
pGEM-T Easy	Ap^r, Lac$^+$, cloning vector	Promega
pSUP202	Ap^r, Tc^r, Cm^r, Mob$^+$, mobilizable suicide vector	[28]
pSUP202*	pSUP202(ΔTc::Km), Ap^r, Km^r, Cm^r, Mob$^+$, mobilizable suicide vector	This work
pSUP2021	pSUP202::Tn*5*, Ap^r, Km^r, Cm^r, source of Km cassette	[28]
pSRA2	Ap^r, Spec^r, Sm^r, source of Sm cassette	[27]
pML5B$^+$	Tc^r, *lacZ*	[25]
pEG276	Gm^r, expression vector	[30]
pEG276-*nasB*	Gm^r, *P. denitrificans nasB* expression construct	This work
pEG276-*nasG*	Gm^r, *P. denitrificans nasG* expression construct	This work

Table 2. NADH- and reduced MV-dependent nitrate and nitrite reductase activity of cytoplasmic fractions prepared from *P. denitrificans* strains affected in *nasB*, *nasG* and *nasC* grown in the presence of nitrate plus glutamate.

Strain	Electron acceptor	Electron donor	
		NADH	MV
WT	NO_3^-	13 ± 4	20 ± 1
	NO_2^-	35 ± 2	203 ± 22
nasC	NO_3^-	n.d.	n.d.
	NO_2^-	39 ± 4	205 ± 20
nasB	NO_3^-	n.d.	13 ± 2
	NO_2^-	n.d.	n.d.
nasG	NO_3^-	n.d.	142 ± 4
	NO_2^-	n.d.	103 ± 7*

Activity units = nmoles·min^{-1}·mg $protein^{-1}$
n.d. = not detectable
* Activity decayed with $t_{1/2}$ of approx. 50 minutes

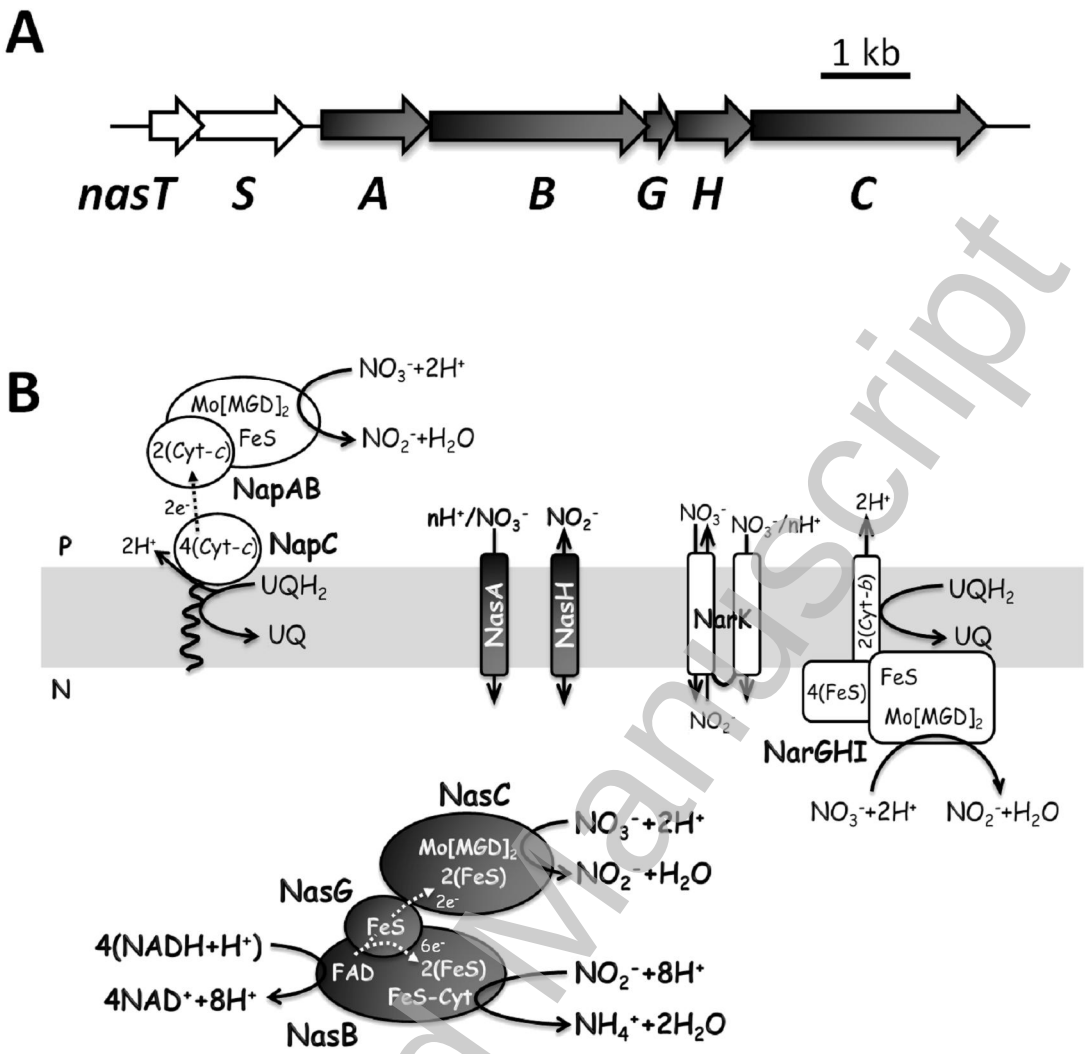

Fig. 1.

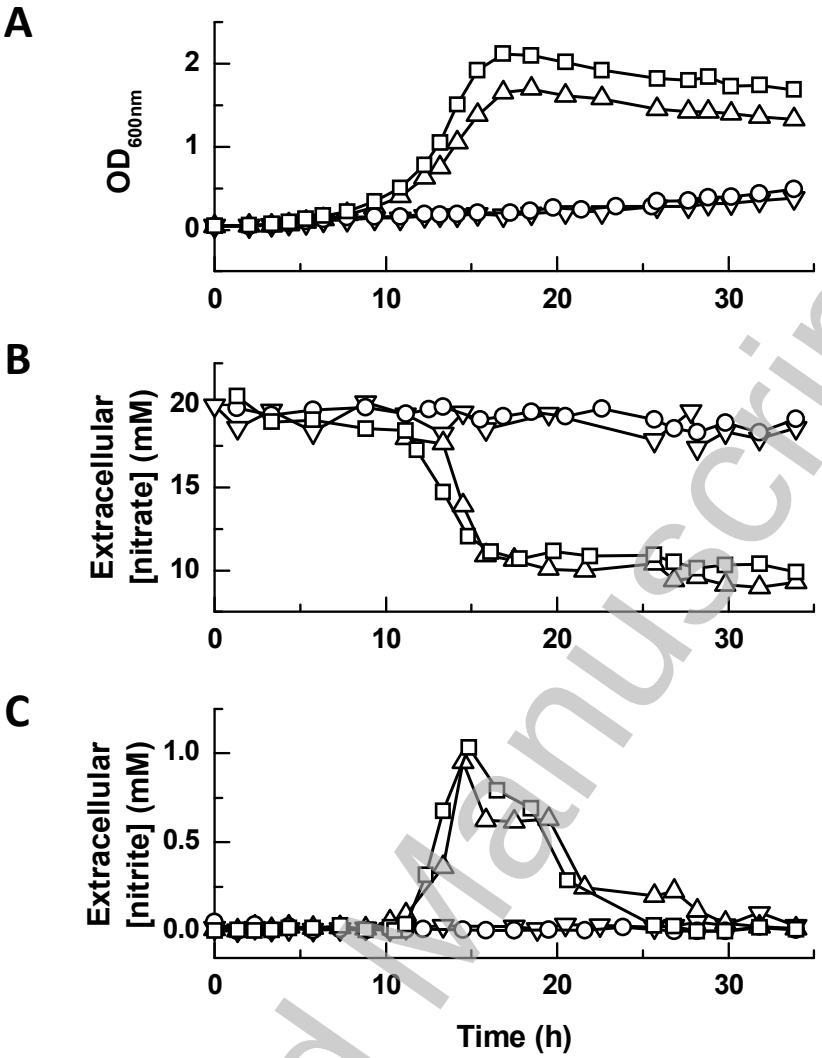

Fig. 2.

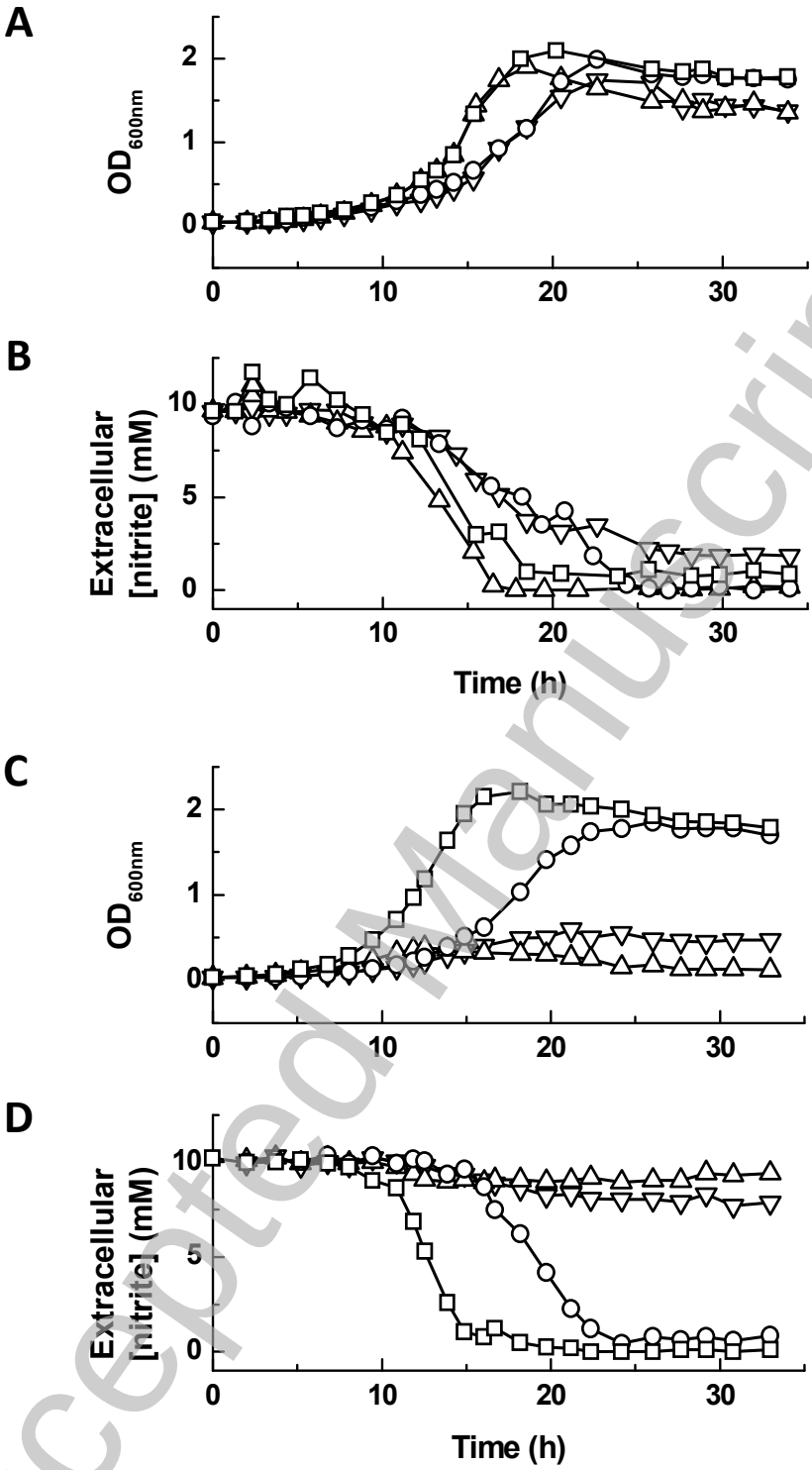

Fig. 3.

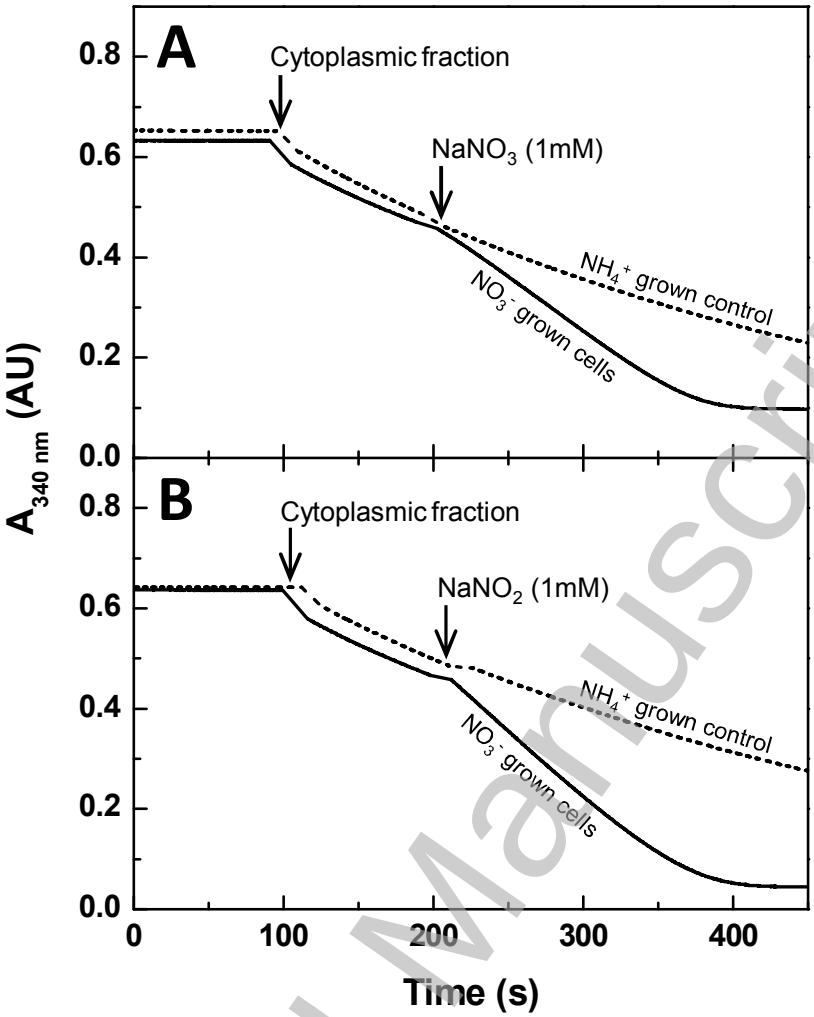

Fig. 4.

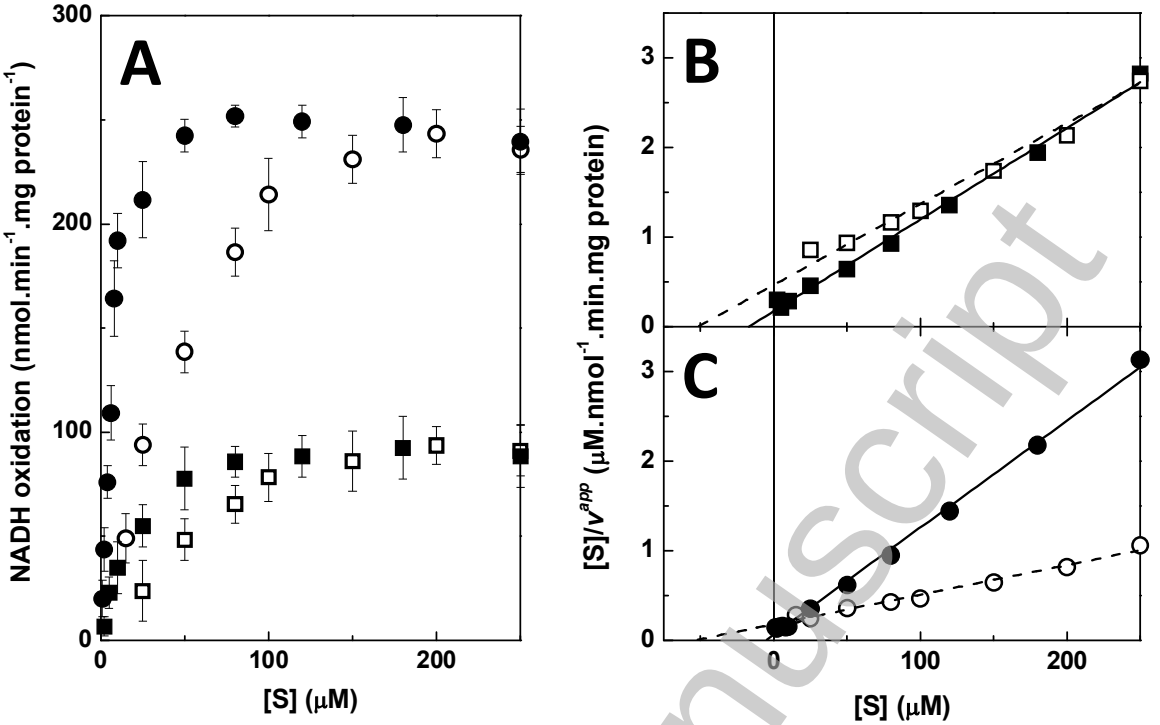

Fig. 5.

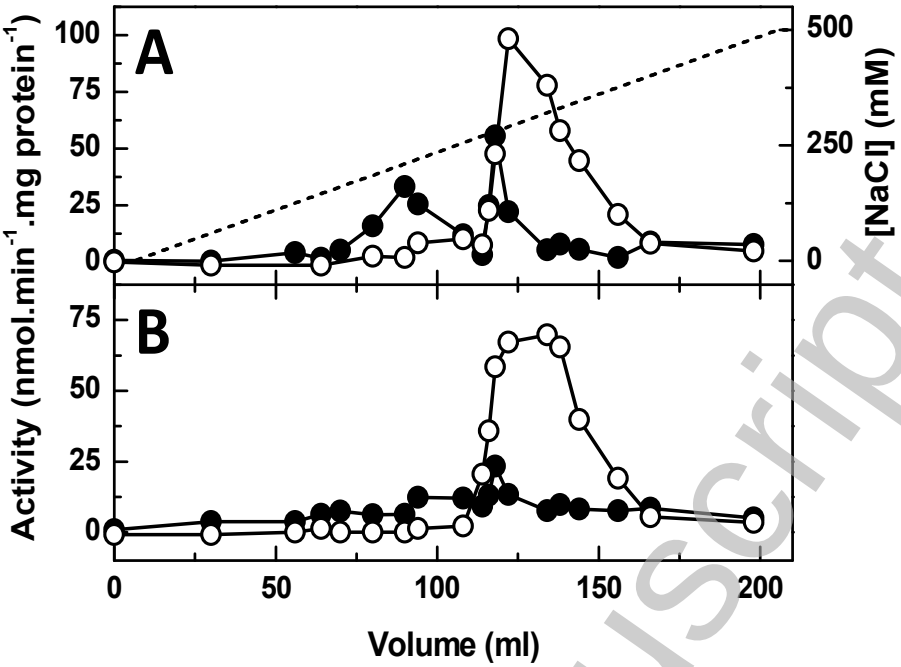

Fig. 6.

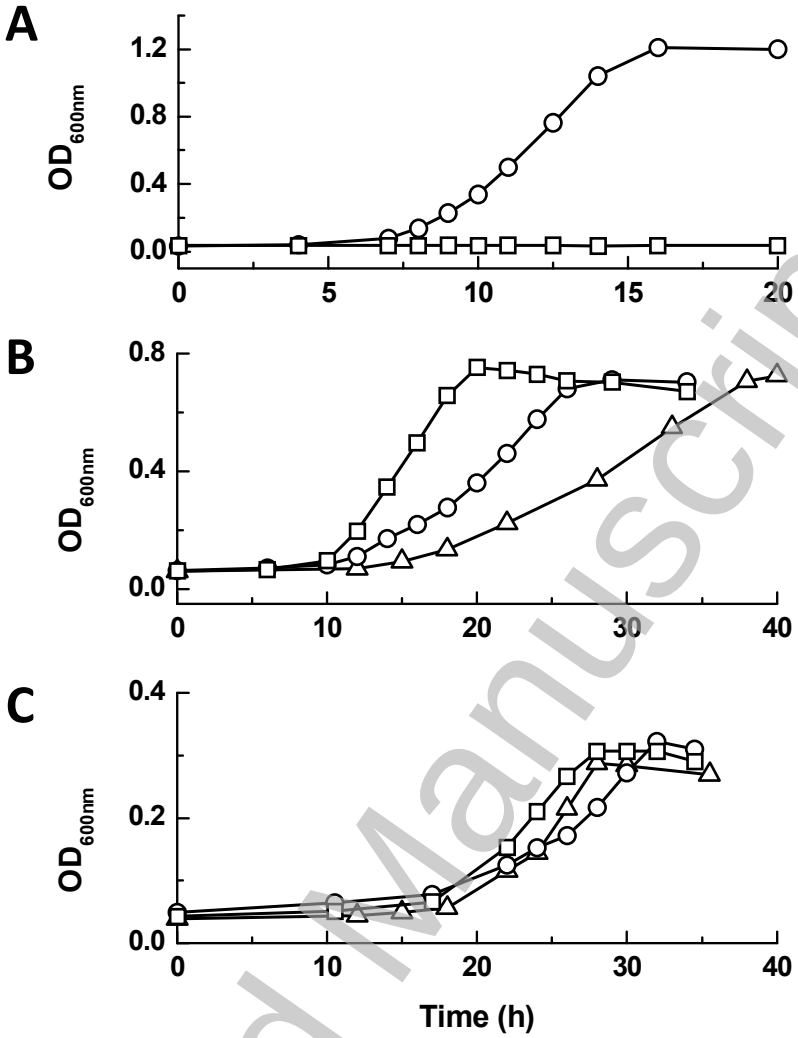

Fig. 7.

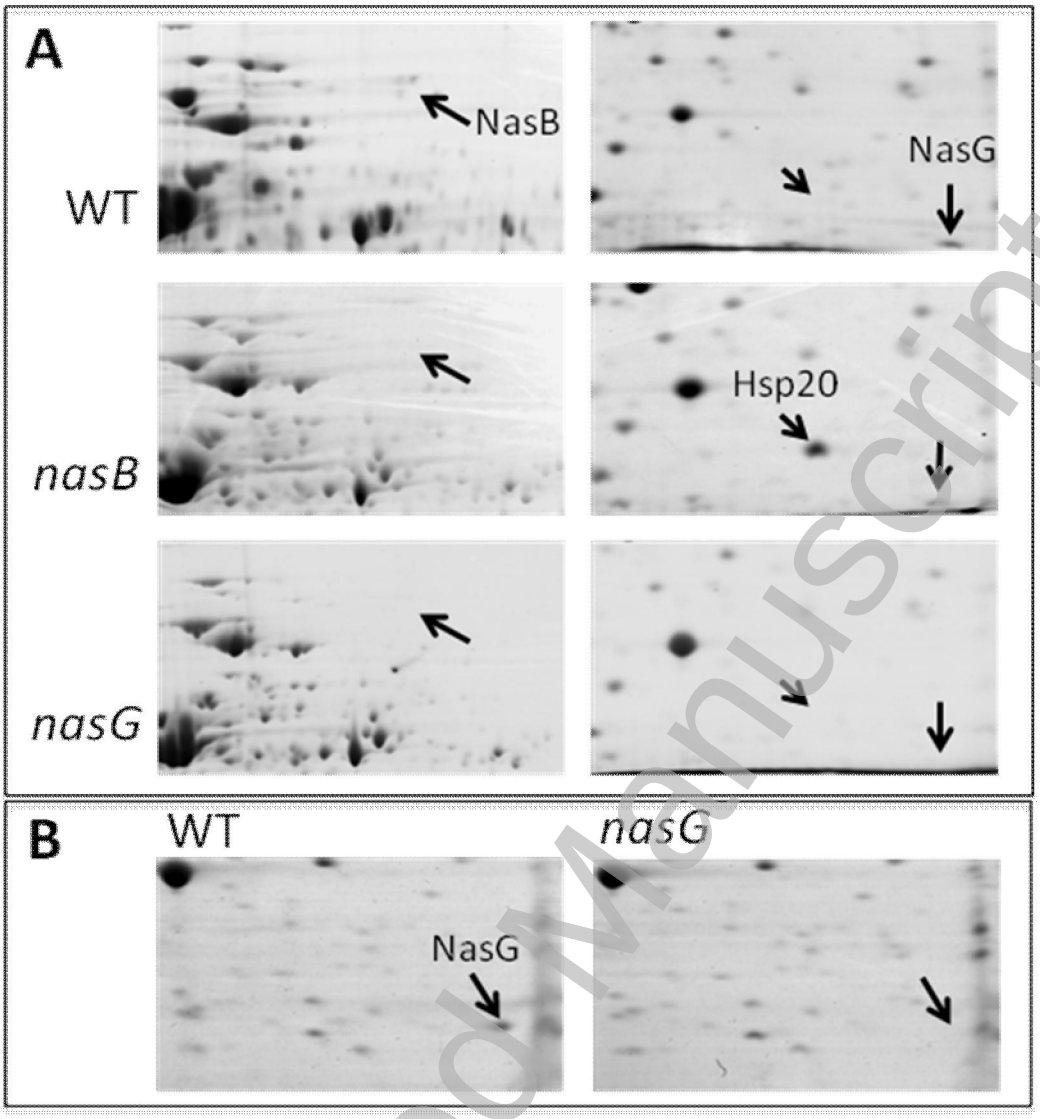

Fig. 8.